

Finite Element Modeling of Plain Weave Fabric from an Un-Woven Initial Yarn Configuration

J. S. Ferranto,¹ and S. Y. Luo

University of Nevada, Reno, USA

¹ jsferranto@yahoo.com

УДК 539.4

Конечноэлементное моделирование тканого материала на основе анализа исходной конфигурации нитей

Дж. С. Ферранто, С. Й. Луо

Университет Невады, Рено, США

Предложена методика прогнозирования прочности тканого материала при растяжении с использованием метода конечных элементов для моделирования переплетений изначально прямых нитей. При оценке прочности и механических характеристик ткани растягивающие усилия прикладываются с пошаговым повышением нагрузки. В данном подходе используются инновационные граничные условия и учитывается несколько уровней симметрии, что позволяет реализовать предложенную модель с помощью стандартных, немодифицированных конечноэлементных пакетов. Поскольку моделируется ткацкий процесс, в качестве исходных данных используются только геометрия и свойства материала нитей, что дает возможность быстро оценить характеристики гипотетических тканей без проведения экспериментов.

Ключевые слова: переплетение нитей, ткань, метод конечных элементов, моделирование.

Introduction. Woven fabrics and flexible composites are an important class of materials with a wide variety of uses. Flexible composites reinforced with woven fabric have many inherently positive characteristics, the potential for high strength, ease of use, and ease of lay-up in the forming process.

Clothing, composite reinforcements, flexible composites, cloth structures, ballistic armors, parachutes, sails and numerous other applications make extensive use of woven fabrics. There is currently a large demand for lightweight military armor made of woven fiber flexible material. Here the large strains allow significantly higher energy absorption and dissipation than a stiff composite, as well as allowing for movement and articulation in the case of body armor. Prior to the curing process many rigid composites behave as flexible composite. The uncured matrix material is liquid and does not affect the structural properties, therefore the flexible woven fabric reinforcement will entirely determine the uncured structural properties. Understanding the mechanics of a composite material with an uncured matrix conforming to a tool shape could improve the lay-up process currently used within industry.

Many biological structures, such as skeletal muscles consisting of striated fiber bundles suspended in an extracellular matrix, may be thought of as wavy fiber flexible composites and modeled accordingly.

Modeling the mechanical behavior of this class of material presents a significant engineering challenge due to the geometric complexity of yarns undulating around each

other. The yarns have a complex shape and may interact with yarns oriented in other directions. Mechanical properties may be both nonlinear and completely different under various loading conditions (uniaxial tension, biaxial tension, shear, bending, etc.).

There are a number of different approaches to modeling the mechanics of woven materials. Modeling approaches are generally classified into three broad categories. Macroscale models treat the fabric as a continuum. Mesoscale models look at the effects of the yarns that are woven around each other, treating the yarns as a continuous material. Microscale models include the effects of the fibers that when bundled together comprise most yarns.

Macroscale analytical models such as the model developed by Peng [1] treat the material as a continuous material with nonlinear orthotropic properties. Macroscale models do not model yarn undulation in the fabric. These models are simple but because they do not fully model yarn interactions, they have difficulties in capturing the effects of crimp interchange and shear angle reorientation. Further these models require time consuming material testing for each fabric to be examined.

Mesoscale analytical models examine a representative volume element (RVE) or unit cell. This is a small piece of the material that can represent the whole using periodic symmetry. These models predict the effects of the yarns and are more likely to closely describe crimp and shear effects. Mesoscale models developed by Assid [2], Barbero [3, 4], Luo [5] and Boljen [6] treat yarn undulation as a sinusoidal function. Crimp interchange is modeled with either Eulerian or Timoshenko based beam bending. These models can be quite accurate, however the underlying assumptions of sinusoidal shape and beam like crimp interchange are not thoroughly tested across a wide range of parameters.

Another common approach to analytical modeling used by Kato [7] and King [8] is to treat each yarn as a series of straight beams pinned together at crossover points. Flattening is modeled with spring elements between intersecting perpendicular yarns. These models have the advantage of simplicity, however they are limited by not modeling realistic yarn undulation shape and mechanics.

FEA modeling techniques are able to more closely match the true physics of fabric mechanics. These models are generally more cumbersome, requiring extensive set up and computer run time. With these models, creating a 3D model of the initial shape of an RVE/unit cell is often the greatest challenge.

Sherburn [9] and Lomov [10, 11] generate 3D models based energy minimization of an assumed shape function for the yarn path. The 3D models can then be used as a basis for mesoscale FEA. They do not account for flattening or cross sectional variations which may cause an incorrect crimp arrangement. Further, the underlying assumption of a shape function is difficult to test across a wide range of parameters. Although they have verified it in certain instances, it is unclear how changes in fabric parameters will affect it.

Tavana [12] and Barbero [3] both utilize mesoscale FEA models of unit cells generated by digitizing photomicrographs of the fabric. Naouar [13] takes a similar approach using X-ray tomography. This approach gives good results but requires photomicrography and analysis. This makes it unsuitable for parametric modeling, or predicting the properties of a fabric before manufacturing.

Hamila [14] used a macroscale FEA model, in which a node exists at each yarn crossover. This method models the yarn reorientation during fabric shear, but has no mechanism to account for crimp interactions or multiaxial loading.

Durville [15] created a microscale FEA model in which individual fibers of each yarn are modeled as beam elements. Contact elements then deform the yarns until the unit cell reaches its initial shape. This method most closely models the real physics of fabric formation and deformation, however it requires finite element software with special algorithms and optimizations for the extremely large amount of contact elements. It is able to make predictions about the deformed shape of the yarn, and the effects of fiber

reorientation within the yarn. It is unclear whether this model will be stable for more complex fabrics or load states.

In this work, we have established a mesoscale FEA model, referred to hereafter as the straight-yarn model, that can predict the shape and mechanical properties of a plain weave fabric based on preformed yarn geometry, that is to say without taking measurements from the woven fabric. Similar to Durville's [15] approach, the model begins with the yarns in a straight configuration, and then deforms the yarns into a woven configuration. The model simulates the effect of the fibrous microstructure by treating the yarn as a transversely orthotropic material. The model is further simplified by taking advantage of the reflective symmetry inherent to a RVE/Unit Cell. With this second symmetry simplification, only one eighth of the RVE needs to be studied. Using these simplifications allows the model to run very quickly with unmodified off the shelf FEA packages, such as ANSYS workbench.

The straight-yarn model described in this paper has a number of advantages.

1. It requires no testing or examination of the fabric, but only the material properties of the pre-woven yarns. Hypothetical fabrics can be easily examined with this approach, allowing fabric properties to be optimized before manufacture.

2. The model inherently predicts the deformation of the yarns including the change in cross section caused by the yarns pressing against each other at the crossover points, i.e., flattening effects, This is entirely without assumptions about the yarn path or crimp relationship.

3. Due to simplified boundary conditions this approach can produce realistic results quickly and easily using standard FEA packages.

1. FEA Modeling.

1.1. **Unit Cells and the Symmetric Modeling Region.** A unit cell or RVE is the smallest piece of a fabric that can represent the entire structure with periodic symmetry. As shown in Fig. 1a, the entire fabric is comprised of these unit cells side by side. For a plain weave fabric a unit cell contains four crossover points. The unit cell still contains reflective symmetry and for modeling purposes it is only necessary to model the shaded region in Fig. 1a. In Fig. 1b one can see the modeling region corresponding to the shaded region in Fig. 1a. Figure 1c shows the modeling region prior to the forming/weaving load step.

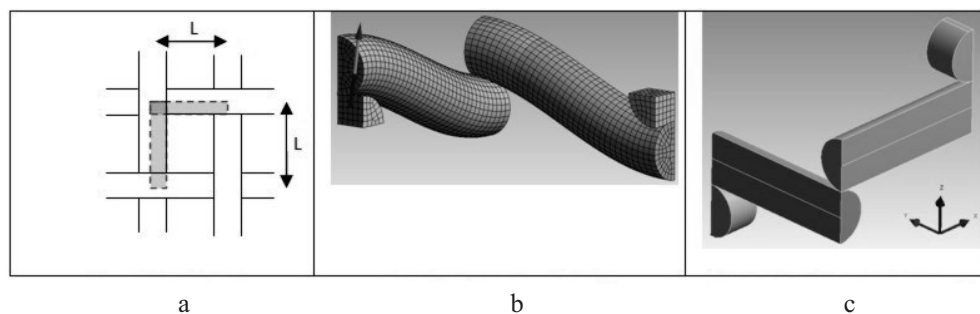


Fig. 1. Unit cell/RVE for plain weave fabric: (a) unit cell; (b) modeling region; (c) pre-woven modeling region.

1.2. **Material Properties.** Fabric yarns commonly consist of bundles of small fibers. Microscale approaches such as Durville et al. [15] examine individual fibers and can use the material properties of the fiber material along with an appropriate contact behavior. Mesoscale models do not include the effects of fiber interaction however Naouar [13] asserts that based on his X-ray tomography studies, fiber bundles may be treated as a continuous material with transversely isotropic properties. The modeling technique in this paper follows the Naouar approach treating fiber bundles as continuous transversely isotropic material. Monofilament yarns may be modeled with standard material properties.

1.3. **Cross Section.** Micrographs show that fiber bundles most commonly assume a lenticular cross section at the yarn contact. This is approximated using an elliptical cross section of the same cross sectional area, and either yarn thickness, width or moment of inertia. Note that the elliptical cross section is applied to the pre-deformed yarn. As the yarn deforms from the straight to the initial position of a fabric, the cross section will be modified by the model.

1.4. **Boundary and Initial Conditions.** Boundary conditions for this model are specifically chosen to follow the actual formation/looming of a woven fabric. In order to model the formation of yarn geometry, we must examine how a loom works.

In all looms, the warp yarns are moved vertically into a shed configuration by some form of heddle or jacquard. As the heddles reorient, wrapping the warp yarn around the weft yarn, the warp is drawn from a spool with a tensioning device. In the direction of the warp yarns, the RVE is free to expand or contract until internal forces find equilibrium with the applied tension.

As the weft yarn is passed through the warp shed (whether by shuttle, rapier, projectile or jet) it is unconstrained. When the heddles reorient the warp yarns, they are pressed into the weft yarns. The RVE is now locked into place through yarn friction. There is likely an unknown tension force in the weft yarn provided by the taught warp yarn, however after removal from the loom the fabric must reorient so as to zero all in plane forces, as required for static equilibrium.

In order to model a RVE as it passes through the loom, we can begin with two perpendicular straight yarns with length S_0 (shown in Fig. 1c). The ends are free to translate in the yarn directions as lateral (crimp) displacement is applied via the loading elements. They will translate until the length of the RVE changes from S_0 to the RVE/unit cell length L_0 . In this model, S_0 and the cross-sectional shape of the yarn are the only required geometric inputs, with L_0 being determined by the model. This allows the model to predict initial fabric shapes with only the yarn geometric parameters known.

The most accessible fabric parameters are the picks/length (n), and the crimp. The picks/length gives the length of the RVE ($n = 1/L_0$). Crimp gives the length of the yarn in the RVE before the loom deforms it, i.e., the straight length ($crimp = S_0/L_0 - 1$). Picks are easily counted, and as crimp is simply the ratio of the length of yarn used to the length of fabric produced it will be well known by the manufacturer. This allows for a simple verification of the model, checking to see if the predicted picks/in are equal to the observed amount in a real fabric.

Observing a plain weave RVE (Fig. 1) it is apparent that the RVE is a symmetric structure (a loom will not apply shear deformation). For this reason, with the appropriate boundary conditions, the fabric RVE may be reduced to a symmetric one eighth model. The symmetric area modeled can be seen in Fig. 1b. Aside from the standard symmetric boundary conditions, this model leaves the two yarns dangling in space. It is necessary to formulate a boundary condition that constrains the Z (normal to the fabric plane) position of these dangling yarns. In Fig. 2, it can be seen that the amplitudes of the two yarns, A_x and A_y , must follow the approximate relationship without considering the flattening effect or other changes in yarn cross section. R_x and R_y are the yarn radii, or one half the yarn thickness for non-circular yarns,

$$A_x + A_y \cong R_x + R_y. \quad (1)$$

Equation (1) is good initial estimate for yarn amplitudes and would hold true if we could assume constant cross section. In reality the yarn amplitudes and diameters are not constant as load is applied. Further as the two yarns bite into each other they may deviate from their initial (unwoven) cross sectional shape. for the FEA model we must define a symmetry parameter that accounts for these variations.

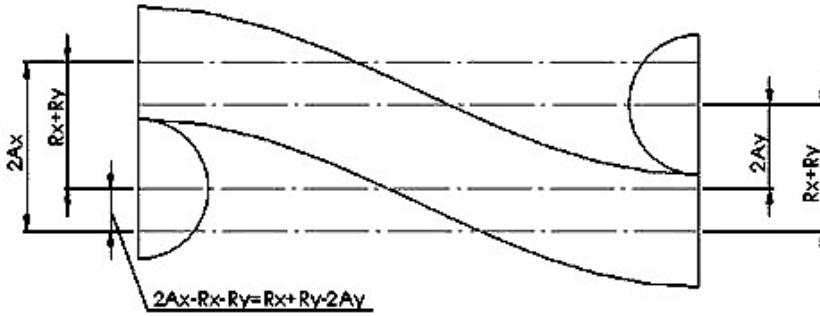


Fig. 2. Approximate relationship between yarn radius and amplitude.

In order to represent the periodicity of a fabric structure a relationship between the amplitudes of the yarns must be maintained. This is approximated by Eq. (1), however, as the yarns may not remain circular at the contact point a generalized parameter must be defined that will determine whether the quarter model is periodically symmetric.

In Fig. 3, if we begin at a yarn crossover point and travel along the yarn paths to the diagonally adjacent crossover point, we can see two paths to follow. If we define the Z direction as normal to the fabric plane, and place the origin at crossover point A we can find the Z position of crossover point B by following either of the two indicated paths. A_x , A_y are the yarn amplitudes and D_{x2} , D_{y2} are the yarn thicknesses.

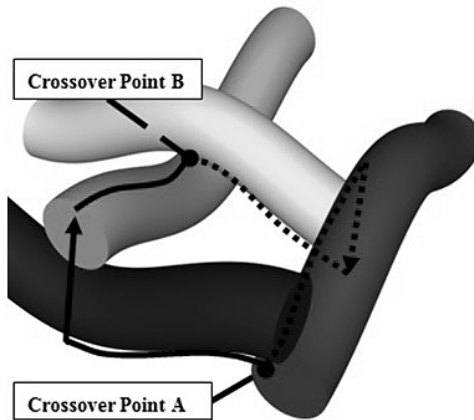


Fig. 3. Eighth model symmetry requirement.

Following the left side path we can see that

$$Z_B = -2A_x + D_{x2} + D_{y2} - 2A_y. \tag{2}$$

Following the right side path we get

$$Z_B = 2A_y - D_{y2} - D_{x2} + 2A_x. \tag{3}$$

Combining Eq. (2) and Eq. (3) yields:

$$Z_B = -Z_B = 0. \tag{4}$$

This indicates that crossover points *A* and *B* have identical *Z* coordinates and are coplanar with the fabric plane. When using a symmetric one eighth model, constraining the dangling crossover points to have identical *Z* coordinates is a necessary symmetric boundary condition.

To maintain the symmetry as the model is reduced to one eighth, an output parameter called distance from symmetry (DFS) is defined as the distance *Z* between points *A* and *B*. When DFS is equal to zero, then the one eighth model will represent a periodic fabric.

Figure 4 shows a yarn configuration with a non-zero DFS. This indicates that it cannot be considered a unit cell of fabric. In order to correct this, lateral displacement must be applied until DFS is equal to zero.

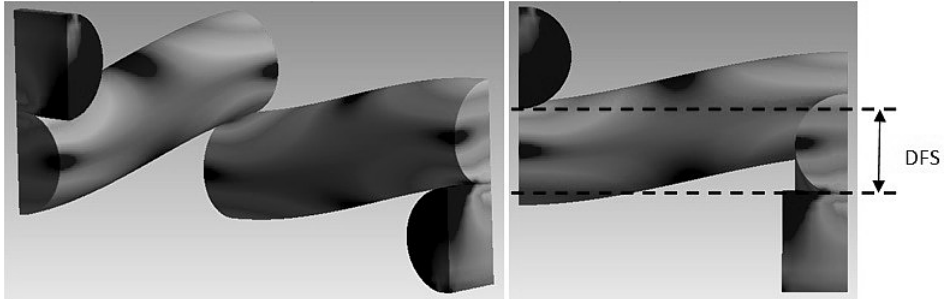


Fig. 4. Distance from symmetry (DFS).

1.5. Loading Elements. In order to apply forces in the most realistic fashion, the model includes loading elements. As shown in Fig. 5, the lateral loading elements used to push the ends into their symmetric position *Z* consist of small portions of the yarn that was removed when converting the model into its one eighth symmetric form. This allows the displacement to be applied in the same fashion as yarns pressing against each other. Applying displacement *Z* with lateral loading elements models yarn flattening at these points allows the previously mentioned DFS to be calculated. The model then iteratively corrects the displacement *Z* applied to the loading elements until the DFS becomes zero.

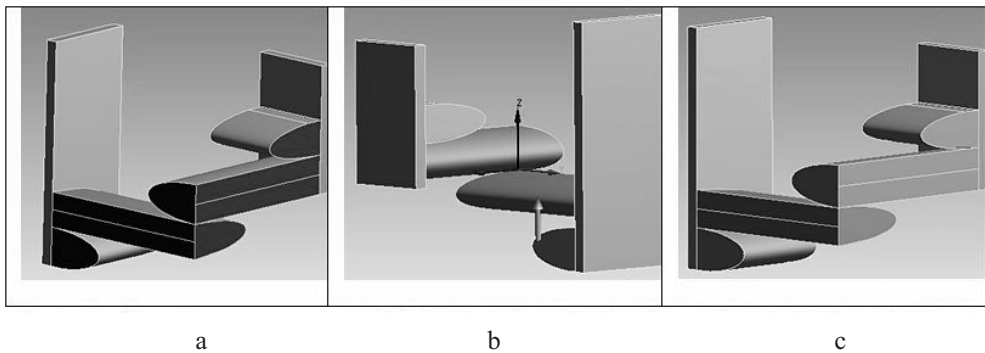


Fig. 5. Boundary conditions, applied loads and loading elements: (a) frictionless support; (b) *Z* displacement (crimp) is applied to the lateral loading elements; (c) tensile force can be applied to rigid bodies with all other DOF constrained (zero tensile force represents the initial shape and is used in the first load step).

1.6. End Conditions/Tensile Loading. In the initial (unloaded) woven condition, there must be no resultant forces in the fabric plane, however the ends of the RVE must be free to deform in the yarn directions. To facilitate this, the end conditions are controlled through

rigid body contact as per Durville [15]. Shown in Fig. 5, rigid bodies are created perpendicular to the yarn at the RVE ends. The rigid bodies are constrained in all degrees of freedom, except translation in the yarn direction. The yarns are then attached to the rigid body through a 'no separation' type contact element. In subsequent load steps, tensile forces may be applied to the rigid body. In this way, the end surfaces maintain the symmetry requirements while allowing the addition of an external tensile force.

1.7. Contact Type, Meshing, and Analysis Settings. Due to the improved boundary conditions, the model is easily able to run with standard auto-meshing. ANSYS 15 auto-mesh with quad/tri elements and a sweep method was used for this study. Element size was allowed small variations in order to optimize mesh quality, however it was commonly between 40 and 60 μm for the fabrics examined.

Frictionless contact was used between yarns, as inter-yarn friction must be zero without an applied shear force. No separation contact was used between the rigid surfaces and the yarns.

Large deformation was used with substeps allowed to range between 10 and 100.

2. Results and Validation. Table 1 shows the properties of the fabrics used to test and validate the straight-yarn model. These fabrics are as reported by Freestone [16] and Barbero [3] in Table 1. D_{x1} and D_{y1} are the yarn widths, D_{x2} and D_{y2} are the yarn thicknesses, $S_{x0'}$ and $S_{y0'}$ are the arc lengths of the woven yarn without external loading.

Table 1

Properties of Test Fabrics

	Material	Freestone	Barbero/CERL
		Saran	Carbon AS4-D
Warp	D_{x1} (mm)	0.259	0.203
	D_{x2} (mm)	0.259	0.630
Weft	D_{y1} (mm)	0.259	0.179
	D_{y2} (mm)	0.259	0.770
Warp	$S_{x0'}$ (mm)	1.709	1.865
Weft	$S_{y0'}$ (mm)	1.603	1.907
Warp	E_x (GPa)	1.00	170.80
	E_y (GPa)	1.00	24.23
Weft	E_x (GPa)	1.00	170.80
	E_y (GPa)	1.00	24.23
	ν	0.350	0.324

2.1. Straight-Yarn Model Residual Inter-Yarn Force (Crimp Force) Validation. As the yarns are deformed from straight to woven configurations, there will be a residual contact force (force perpendicular to the fabric plane, at the crossover points) remaining in the weave. In reality, this forming force may remain as an internal force, or it may experience a stress relaxation effect. In order to examine this, a monofilament saran weave was generated with the model. The saran was deformed into its initial configuration, and then the crimp (yarn amplitude, d) was varied. This is compared to a second model in which the same saran weave was deformed into the woven configuration, then the geometry is exported as a parasolid to a new model, thus zeroing all internal forces, before

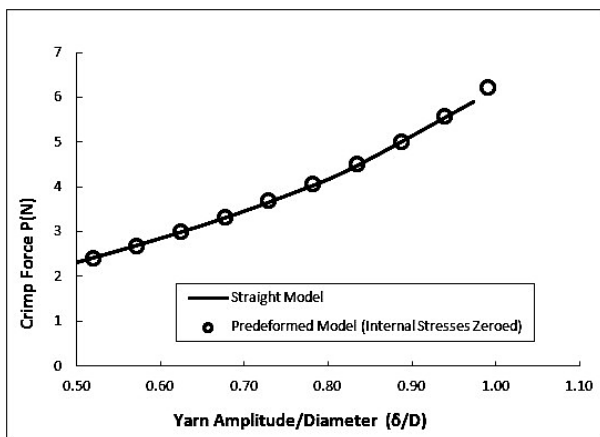


Fig. 6. Initial inter-yarn contact force.

adjusting the crimp. As shown in Fig. 6, each model produces identical results after the crimp force (P) has been normalized. This indicates that residual crimp forces will have no effect on the shape or behavior of the fabric.

2.2. *Freestone Stress–Strain Curves.* The straight-yarn model was used to recreate experiments performed by Freestone et al. [16]. Results indicate a close correlation between Freestone’s experiments and the straight-yarn model. Freestone’s experiments involved a monofilament saran yarn, and tension was applied in several multiaxial load states. Figure 7 shows the stress strain curve for pure biaxial tension as well as a mixed state where the y stress is twice the x stress. N_x and N_y refer to applied fabric stress, that is force per length of fabric.

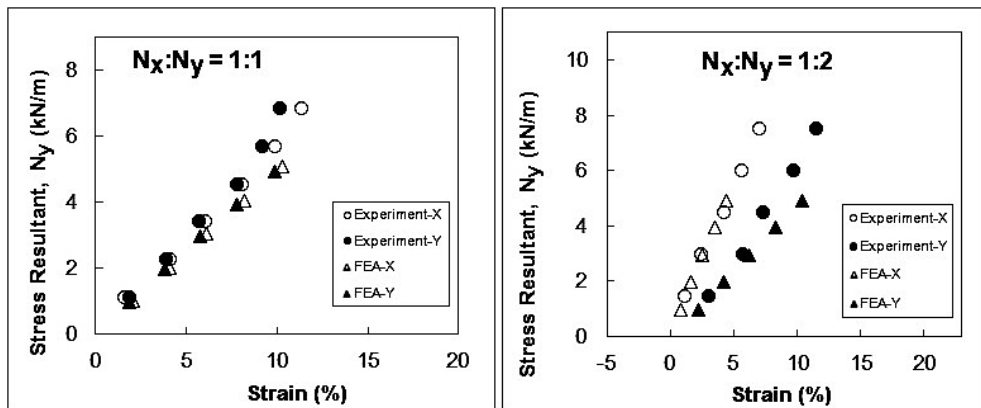


Fig. 7. Freestone stress–strain curves compared to straight-yarn model (FEA).

2.3. *Experimental Patterns (from Barbero [3]).* The straight-yarn model was used to generate the initial shape of a fabric tested by CERL and reported by Barbero et al. [4]. CERL measured, with photomicrography, the initial shape of yarns in an AS4/vinylester plain weave fabric. The fibrous construction of the yarns was simulated using transversely isotropic material properties as per Barbero [3] and Naouar [13]. The cross section of the CERL yarn can be seen to be lenticular and is approximated with an ellipse. Figure 8 shows that the straight-yarn model FEA approach gives a shape nearly identical to the micrograph from CERL.

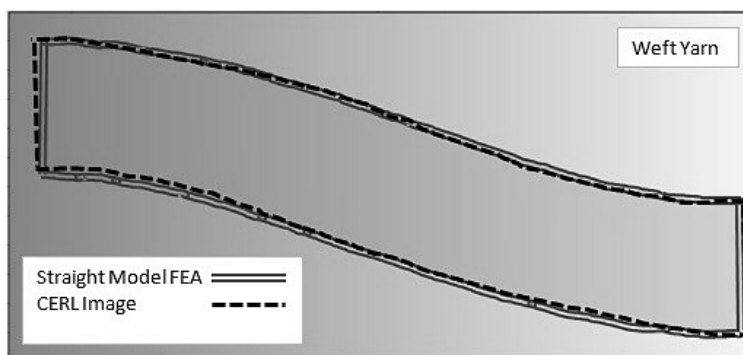


Fig. 8. Straight-yarn model weft yarn superimposed on Barbero/CERL [3] yarn.

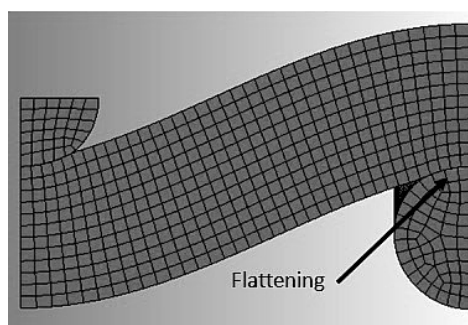


Fig. 9. Yarn flattening.

2.4. Yarn Flattening. In Fig. 9, the effect of flattening can be seen in a hypothetical saran fabric. An inherent advantage to the straight yarn model is that it models the fabric forming/weaving process and therefore includes the effect of yarn flattening where the two yarns bite into each other.

Conclusions. A technique using standard unmodified FEA software to determine the initial shape and tensile behavior of plain weave fabric has been developed and verified. This method models mesoscale unit cells of plain weave to a high degree of accuracy. By taking advantage of symmetries within the unit cell/RVE the straight yarn model can be run on standard off the shelf FEA packages without special optimization algorithms. Using only information about the fibers, yarns and weaving method, the FEA based straight-yarn modeling technique can quickly and easily determine the shape and tensile behavior of fabrics as well as predict yarn flattening without a requirement for fabric testing and characterization. The technique can be used to verify or calibrate theoretical fabric models and to design fabrics with properties tuned to specific applications, e.g., the prediction of long-term deformations in woven materials using the relations of linear and nonlinear viscoelasticity, as in [17].

Резюме

Запропоновано методикку прогнозування міцності тканого матеріалу при розтягуванні з використанням методу скінченних елементів для моделювання переплетень початково прямих ниток. При оцінці міцності і механічних характеристик тканини розтяжні зусилля прикладаються з покроковим підвищенням навантаження. У даному підході використовуються інноваційні граничні умови і враховується кілька рівнів

симетрії, що дозволяє реалізувати запропоновану модель за допомогою стандартних, немодифікованих скінченноелементних пакетів. Оскільки моделюється ткацький процес, як вихідні дані використовуються лише геометрія та властивості матеріалу ниток, що дозволяє швидко оцінити характеристики гіпотетичних тканин без проведення експериментів.

1. X. Peng, Z. Guo, and T. Du, "A simple anisotropic hyperelastic constitutive model for textile fabrics with application to forming simulation," *Composites Part B – Engineering*, **52**, 275–281 (2013).
2. M. Assid, B. Boubaker, and J. F. Ganghoffer, "Equivalent properties of monolayer fabric from mesoscopic modelling strategies," *Int. J. Solids Struct.*, **48**, No. 20, 2920–2930 (2011).
3. E. J. Barbero, J. Trovillion, and J. A. Mayugo, "Finite element modeling of plain weave fabrics from photomicrograph measurements," *Compos. Struct.*, **73**, No. 1, 41–52 (2005).
4. E. J. Barbero, T. M. Damiani, and J. Trovillion, "Micromechanics of fabric reinforced composites with periodic microstructure," *Int. J. Solids Struct.*, **42**, No. 9-10, 2489–2504 (2004).
5. S. Y. Luo and A. Mitra, "Finite elastic behavior of flexible fabric composite under biaxial loading," *J. Appl. Mech.*, **66**, No. 3, 631–638 (1999).
6. M. Boljen and S. Hiermaier, "Continuum constitutive modeling of woven fabric," *The European Physical Journal Special Topics*, **206**, No. 1, 149–161 (2012).
7. S. Kato, T. Yoshino, and H. Minami, "Formulation of constitutive equations for fabric membranes based on the concept of fabric lattice model," *Eng. Struct.*, **21**, No. 8, 691–708 (1999).
8. M. J. King, P. Jearanaisilawong, and S. Socrate, "A continuum constitutive model for the mechanical behavior of woven fabrics," *Int. J. Solids Struct.*, **42**, No. 13, 3867–3896 (2005).
9. M. Sherburn, A. Long, and A. Jones, "Prediction of textile geometry using an energy minimization approach," *J. Industr. Textil.*, **41**, No. 4, 345–369 (2010).
10. S. V. Lomov, T. Mikolanda, and M. Kosek, "Model of internal geometry of textile fabrics: data structure and virtual reality implementation," *J. Textil. Inst.*, **98**, No. 1, 1–13 (2007).
11. S. V. Lomov, A. V. Truevtzev, and C. Cassidy, "Predictive model for the fabric-to-yarn bending stiffness ratio of a plain-woven set fabric," *Textil. Res. J.*, **70**, No. 12, 1088–1096 (2000).
12. R. Tavana, S. S. Najar, and M. T. Abadi, "Meso/macro-scale finite element model for forming process of woven fabric reinforcements," *J. Compos. Mater.*, **47**, No. 17, 2075–2085 (2013).
13. N. Naouar, E. Vidal-Salle, and J. Schneider, "Meso-scale FE analyses of textile composite reinforcement deformation based on X-ray computed tomography," *Compos. Struct.*, **116**, 165–176 (2014).
14. N. Hamila and P. Boisse, "Tension locking in finite-element analyses of textile composite reinforcement deformation," *Comptes Rendus Mecanique*, **341**, No. 6, 508–519 (2013).
15. D. Durville, "Simulation of the mechanical behaviour of woven fabrics at the scale of fibers," *Int. J. Mater. Form.*, **3**, No. 2, S1241–S1251 (2010).

16. W. D. Freestone, M. M. Platt, and M. M. Schoppee, "Mechanics of elastic performance of textile materials Part XVIII. Stress-strain response of fabrics under two dimensional loading," *Textil. Res. J.*, **37**, No. 11, 948–975 (1967).
17. E. L. Danil'chuk, "Modeling of creep of polymer woven fabrics," *Strength Mater.*, **46**, No. 6, 794–800 (2014).

Received 11. 04. 2015